

# Accepted Manuscript



Bundle Branch Reentrant Ventricular Tachycardia: Novel Genetic Mechanisms in a Life-Threatening Arrhythmia

Jason D. Roberts, MD MAS, Michael H. Gollob, MD, Charlie Young, MD, Sean P. Connors, MD DPhil, Chris Gray, MD, Stephen B. Wilton, MD MSc, Martin S. Green, MD, Dennis W. Zhu, MD, Kathleen A. Hodgkinson, PhD, Annie Poon, PhD, Qiuju Li, MSc, Nathan Orr, BSc, Anthony S. Tang, MD, George J. Klein, MD, Julianne Wojciak, MSc, Joan Campagna, CCMA, Jeffrey E. Olgin, MD, Nitish Badhwar, MBBS, Vasanth Vedantham, MD PhD, Gregory M. Marcus, MD MAS, Pui-Yan Kwok, MD PhD, Rahul C. Deo, MD PhD, Melvin M. Scheinman, MD

PII: S2405-500X(16)30392-9

DOI: [10.1016/j.jacep.2016.09.019](https://doi.org/10.1016/j.jacep.2016.09.019)

Reference: JACEP 293

To appear in: *JACC: Clinical Electrophysiology*

Received Date: 2 September 2016

Revised Date: 27 September 2016

Accepted Date: 29 September 2016

Please cite this article as: Roberts JD, Gollob MH, Young C, Connors SP, Gray C, Wilton SB, Green MS, Zhu DW, Hodgkinson KA, Poon A, Li Q, Orr N, Tang AS, Klein GJ, Wojciak J, Campagna J, Olgin JE, Badhwar N, Vedantham V, Marcus GM, Kwok P-Y, Deo RC, Scheinman MM, Bundle Branch Reentrant Ventricular Tachycardia: Novel Genetic Mechanisms in a Life-Threatening Arrhythmia, *JACC: Clinical Electrophysiology* (2016), doi: 10.1016/j.jacep.2016.09.019.

This is a PDF file of an unedited manuscript that has been accepted for publication. As a service to our customers we are providing this early version of the manuscript. The manuscript will undergo copyediting, typesetting, and review of the resulting proof before it is published in its final form. Please note that during the production process errors may be discovered which could affect the content, and all legal disclaimers that apply to the journal pertain.

## Bundle Branch Reentrant Ventricular Tachycardia: Novel Genetic Mechanisms in a Life-Threatening Arrhythmia

Jason D. Roberts, MD MAS<sup>\*,y</sup>; Michael H. Gollob, MD<sup>z</sup>; Charlie Young, MD<sup>x</sup>; Sean P. Connors, MD DPhil<sup>ij</sup>; Chris Gray, MD<sup>l</sup>; Stephen B. Wilton, MD MSc<sup>#</sup>; Martin S. Green MD<sup>yy</sup>; Dennis W. Zhu MD<sup>zz</sup>; Kathleen A. Hodgkinson, PhD<sup>\*\*</sup>; Annie Poon, PhD<sup>xx</sup>; Qiuju Li, MSc<sup>z</sup>; Nathan Orr, BSc<sup>z</sup>; Anthony S. Tang, MD<sup>\*</sup>; George J. Klein, MD<sup>\*</sup>; Julianne Wojciak, MSc<sup>y</sup>; Joan Campagna, CCMA<sup>y</sup>; Jeffrey E. Olgin, MD<sup>y</sup>; Nitish Badhwar, MBBS<sup>y</sup>; Vasanth Vedantham, MD PhD<sup>y</sup>; Gregory M. Marcus, MD MAS<sup>y</sup>; Pui-Yan Kwok, MD PhD<sup>xx</sup>; Rahul C. Deo, MD PhD<sup>xx,{{</sup>; Melvin M. Scheinman MD<sup>y</sup>

<sup>\*</sup>Section of Cardiac Electrophysiology, Division of Cardiology, Department of Medicine, Western University, London, Ontario, Canada.

<sup>y</sup>Section of Cardiac Electrophysiology, Division of Cardiology, Department of Medicine, University of California San Francisco, San Francisco, California, USA.

<sup>z</sup>Peter Munk Cardiac Centre, Toronto General Hospital, University of Toronto, Toronto, ON, Canada.

<sup>x</sup>Section of Cardiac Electrophysiology, Division of Cardiology, Department of Medicine, Santa Clara Kaiser Medical Center, Santa Clara, California, USA.

<sup>ij</sup>Section of Cardiac Electrophysiology, Division of Cardiology, Department of Medicine, Memorial University, St. John's, Newfoundland, Canada.

<sup>l</sup>Section of Cardiac Electrophysiology, Division of Cardiology, Department of Medicine, Dalhousie University, Halifax, Nova Scotia, Canada.

<sup>#</sup>Libin Cardiovascular Institute of Alberta, Cumming School of Medicine, University of Calgary, Calgary, Alberta, Canada.

<sup>yy</sup>Section of Cardiac Electrophysiology, Division of Cardiology, Department of Medicine, University of Ottawa Heart Institute, Ottawa, Ontario, Canada.

<sup>zz</sup>Cardiac Electrophysiology Laboratories, Regions Hospital, St. Paul, Minnesota; Department of Medicine, University of Minnesota, Minneapolis, Minnesota.

<sup>\*\*</sup>Faculty of Medicine, Memorial University, St. John's, Newfoundland, Canada.

<sup>xx</sup>Cardiovascular Research Institute, University of California San Francisco, San Francisco, California, USA.

<sup>{{</sup>Department of Medicine, California Institute for Quantitative Biosciences and Institute for Human Genetics, University of California San Francisco, San Francisco, California, USA.

**Short Title:** Genetic Mechanisms of BBRVT

**Funding Sources:** J.D.R. was supported by the George Mines Travelling Fellowship Grant from the Canadian Heart Rhythm Society during this study. M.H.G. is supported by a Mid-Career Investigator Award from the Heart and Stroke Foundation of Ontario. M.M.S. is supported by the Deb philanthropic fund.

**Disclosures:** None.

### Corresponding Author:

Jason D Roberts, MD MAS

339 Windermere Road, B6-129B, London, ON, Canada, N6A 5A5

Phone: (519) 663-3746; Ext: 34526 ; Fax: (519) 663-3782 ; Email: [jason.roberts@lhsc.on.ca](mailto:jason.roberts@lhsc.on.ca)

**Abstract**

**Background** Bundle branch reentrant ventricular tachycardia (BBRVT) is a life-threatening arrhythmia occurring secondary to macroreentry within the His-Purkinje system. Although classically associated with dilated cardiomyopathy, BBRVT may also occur in the setting of isolated, unexplained conduction system disease.

**Objective** We sought to investigate for an underlying genetic etiology in cases of apparent idiopathic BBRVT.

**Methods** Cases of BBRVT with normal biventricular size and function were recruited from 6 North American centers. Enrollment required a clinically documented wide complex tachycardia and BBRVT proven during invasive electrophysiology study. Study participants were screened for mutations within genes associated with cardiac conduction system disease. Pathogenicity of identified mutations was evaluated using *in silico* phylogenetic and physicochemical analyses and *in vitro* biophysical studies.

**Results** Among 6 cases of idiopathic BBRVT, each presented with hemodynamic compromise and 2 suffered cardiac arrests requiring resuscitation. Putative culprit mutations were identified in 3 of 6 cases, including 2 in *SCN5A* (Ala1905Gly [novel] and c.4719C>T [splice site mutation]) and 1 in *LMNA* (Leu327Val [novel]). Biophysical analysis of mutant Ala1905Gly Na<sub>v</sub>1.5 channels in tsA201 cells revealed significantly reduced peak current density and positive shifts in the voltage-dependence of activation, consistent with a loss-of-function. The *SCN5A* c.4719C>T splice site mutation has previously been reported as disease causing in 3 cases of Brugada syndrome, while the novel *LMNA* Leu327Val mutation was associated with a classic laminopathy phenotype. Following catheter ablation, BBRVT was non-inducible in all cases and none experienced a clinical recurrence during follow-up.

**Conclusions** Our investigation into apparent idiopathic BBRVT has identified the first genetic culprits for this life-threatening arrhythmia, providing further insight into its underlying pathophysiology and emphasizing a potential role for genetic testing in this condition. Our findings also highlight BBRVT as a novel genetic etiology of unexplained sudden cardiac death that can be cured with catheter ablation.

**Key Words:** ventricular tachycardia, genetics, sudden cardiac death, conduction system disease

### **Condensed Abstract**

Bundle branch reentrant ventricular tachycardia (BBRVT) is a life-threatening arrhythmia occurring secondary to macroreentry within the His-Purkinje system. Our limited insight into its pathogenesis is highlighted by apparent idiopathic cases that develop in the setting of unexplained conduction system disease. Among 6 cases of idiopathic BBRVT that were screened, we identified 3 that possessed culprit genetic mutations, including 2 in *SCN5A* (cardiac sodium channel) and 1 in *LMNA* (Lamin A/C). These cases reveal that BBRVT is a genetic condition and introduce the arrhythmia as a novel genetic cause of unexplained sudden cardiac death that is curable with catheter ablation.

### **Abbreviations List**

BBRVT = bundle branch reentrant ventricular tachycardia, ECG = electrocardiogram, EPS = electrophysiology study, H = His bundle signal, V = ventricular activation, WT = wild-type, BrS = Brugada syndrome.

## Introduction

Bundle branch reentrant ventricular tachycardia (BBRVT) is a life-threatening arrhythmia characterized by macroentry within the His-Purkinje system (1). The BBRVT circuit most often consists of antegrade conduction along the right bundle branch followed by trans-septal intra-myocardial conduction and retrograde conduction along the left bundle branch (**Figure 1a**) (2). This manifests as a left bundle branch block pattern on the surface electrocardiogram (ECG), although a right bundle branch block pattern may also be observed when circuit propagation is in the opposite direction (**Figure 1b**) (3). The hallmark finding of BBRVT on invasive electrophysiology study (EPS) distinguishing it from myocardial VT is the presence of a His bundle signal (H) preceding ventricular activation (V), with changes in the H-H interval driving changes in the V-V interval (**Figure 1c**) (3).

Findings common to patients with BBRVT in initial studies included the presence of a prolonged HV-interval, along with structural heart disease, most often in the form of dilated cardiomyopathy (3). Subsequent reports emerged documenting BBRVT in the absence of structural heart disease, suggesting that conduction system disease in isolation may be sufficient for arrhythmia development (4, 5). Notably, many of the patients with BBRVT and structurally normal hearts were young and otherwise healthy, spawning curiosity into the underlying etiology responsible for their predisposition to the arrhythmia (4).

Conduction system disease, a feature common to all cases of BBRVT, is increasingly appreciated to have an underlying genetic etiology, particularly among individuals less than 60 years of age (6–8). Given that His-Purkinje disease may provide a sufficient substrate for BBRVT in isolation, we hypothesized that mutations within genes implicated in conduction system disease may serve as the underlying culprits for cases of apparent idiopathic BBRVT.

## Methods

### Study Population

Individuals less than 60 years of age with BBRVT in the absence of cardiomyopathy were recruited from 6 North American medical centers. Enrollment required a clinically documented wide complex tachycardia and confirmation of normal biventricular size and function with echocardiography and/or cardiac magnetic resonance imaging. BBRVT had to be successfully induced at the time of invasive EPS. Individuals with a medical disorder known to cause conduction system disease, including muscular dystrophies associated with heart block, specific forms of myocarditis (Lyme and giant cell), and sarcoidosis were excluded. Participant demographics and medical details were obtained through review of medical records. Individuals who did not have a genetic culprit identified as part of their clinical care underwent genetic testing as part of a research protocol and provided signed informed consent approved by the University of California, San Francisco Committee on Human Research.

### Electrophysiology Study and Catheter Ablation

Invasive EPS and BBRVT ablations were performed as described previously (9, 10). In the event that standard programmed extra-stimulation was unsuccessful for induction, long-short extra-stimuli were used. Full details regarding the EPS, criteria to confirm the diagnosis of BBRVT, and ablation procedure are provided in the **Online Supplement**.

### Genetic Analysis

Two of the six patients had commercial genetic testing (Ambry Genetics, CA, USA and DNA Diagnostic Laboratory, University of Colorado Denver, CO, USA) as part of their clinical workup. The remaining 4 individuals were screened for mutations using a next-generation sequencing panel containing 12 genes previously implicated in conduction system disease

(*SCN5A*, *SCN10A*, *SCN1B*, *TRPM4*, *GJA1*, *LMNA*, *TBX5*, *NKX2-5*, *PRKAG2*, *KCNK3*, *KCNK17*, and *HCN4*). Details regarding genomic DNA extraction, gene capture, library preparation, sequencing, and bioinformatic analysis are provided in the **Online Supplement**.

#### *In Silico* Mutation Analysis

Prevalence of identified mutations was assessed using the Exome Aggregation Consortium (<http://exac.broadinstitute.org>). Evaluation of sequence conservation across species was performed using the NCBI HomoloGene database (<https://www.ncbi.nlm.nih.gov/homologene/>) and the UCSC Genome Browser (<https://genome.ucsc.edu/>). *In silico* prediction of the functional effects of missense mutations was examined using Polymorphism Phenotyping v2 (PolyPhen-2) ([genetics.bwh.harvard.edu/pph2/](http://genetics.bwh.harvard.edu/pph2/)), Sorting Intolerant From Tolerant (SIFT) ([sift.jcvi.org](http://sift.jcvi.org)), and Mutation Taster (<http://www.mutationtaster.org/>). The impact of the putative *SCN5A* splice site mutation was evaluated using the Splice Site Prediction by Neural Network ([www.fruitfly.org/seq\\_tools/splice.html](http://www.fruitfly.org/seq_tools/splice.html)), Human Splicing Finder ([www.umd.be/HSF/](http://www.umd.be/HSF/)) tools, and Mutation Taster.

#### Electrophysiological Studies of *SCN5A* Ala1905Gly

The *SCN5A* Ala1905Gly mutation was introduced into a wild-type (WT) *SCN5A* pcDNA1 clone using the QuickChange site directed mutagenesis kit (Stratagene, CA, USA) and confirmed with bidirectional Sanger sequencing. Transmembrane Na<sub>v</sub>1.5 currents were recorded using the whole cell patch clamp technique at room temperature using an Axopatch 200B amplifier (Axon Instruments, CA, USA), while voltage-clamp command pulses were generated using pCLAMP software v8.0 (Axon Instruments). Data was acquired and analyzed with the pClamp10 and Clampfit software programs, respectively (Axon Instruments). Additional details

regarding wild-type and mutant *SCN5A* expression in tsA201 cells and electrophysiological analysis are provided in the **Online Supplement**.

### Statistical Analysis

Normally distributed continuous variables are presented as means  $\pm$  standard deviation for clinical data and means  $\pm$  standard error for the electrophysiological measurements from patch clamping. Comparison of continuous variables was performed using Student's t-tests. Statistical analyses were performed using GraphPad Prism5. Two-tailed p-values  $< 0.05$  were considered statistically significant.

## **Results**

### Clinical Cases

#### *Clinical Features*

Six cases of BBRVT were identified in individuals less than 60 years of age with normal biventricular size and function. The mean age at diagnosis was  $26.8 \pm 9.3$  years (range: 17-38) and 4 were male (**Table 1**). Genetic culprits were identified in Case 1 (*SCN5A* Ala1905Gly), Case 2 (*SCN5A* c.4719C>T), and Case 3 (*LMNA* Leu327Val). Two of the 6 cases initially presented with intermittent third degree atrioventricular block and subsequently developed BBRVT within days of their sentinel event (Cases 4 and 5; the clinical aspects of Case 5 have been previously reported(11)) (**Table 1**). Notably, both had bicuspid aortic valves documented on echocardiography and heavy calcification was observed in Case 5, while only valvular thickening was present in Case 4. A single patient had a longstanding history of persistent atrial fibrillation diagnosed at 28 years of age (Case 3) (**Table 1**). None of the remaining cases had any evidence of structural heart disease or prior cardiac history. Of the 4 cases that presented with BBRVT, 2 suffered cardiac arrests requiring resuscitation, one had syncope, and one had



palpitations (**Table 1**). Case 3 had a brother that required permanent pacemaker insertion at 52 years of age for sinus node dysfunction, while there was no family history of other arrhythmic issues, including unexplained premature sudden cardiac death, in any of the remaining cases.

### *Surface ECG*

Evidence of conduction system disease on surface ECG was present in 4 of the 6 patients at baseline in the absence of BBRVT (Cases 3-6; **Table 1** and **Figure 2**). Although Case 1 exhibited mild QRS prolongation (120 ms) and Case 2 had an indeterminate axis, neither had definitive findings consistent with conduction system disease. As highlighted above, Cases 4 and 5 presented with third degree atrioventricular block and had wide-complex infra-nodal escape rhythms (**Figure 3**). Patient 3 had a history of persistent atrial fibrillation in association with a non-specific intra-ventricular conduction delay, while Case 6 had incomplete right bundle branch block (**Table 1** and **Figure 2**). Aside from the calcification observed in association with the bicuspid aortic valve in Case 5, which may predispose to Lev's disease, there were no other known etiologies that could account for the observed conduction system disease in the study participants.

### *Electrophysiology Study*

All patients underwent invasive EPS and all had a prolonged HV at baseline (mean: 69.2  $\pm$  9.1 ms) (**Table 1**). BBRVT was induced in all cases with programmed extra-stimulation (**Figure 4a**). BBRVT during EPS had right and left bundle branch block morphologies in Cases 1 and 5 (**Supplemental Figure 1**), while only a left-bundle branch block morphology was observed in the remaining 4 individuals (**Supplemental Figure 1**). The cycle length of BBRVT ranged from 350 ms (171 beats per minute [bpm]) to 220 ms (273 bpm) and in each patient was associated with marked symptoms and varying degrees of hemodynamic instability. In each case

of BBRVT, AV dissociation was observed and changes in either the H-H or right bundle-right bundle potentials were observed to precede and predict changes in subsequent V-V intervals (**Figure 4b**). All patients were treated with catheter ablation of the right bundle branch, which rendered tachycardia non-inducible.

### *Follow-Up*

Following catheter ablation, there was no recurrence of VT in any of the cases (mean follow-up:  $6.7 \pm 4.6$  years) (**Table 1**). Patient 1 developed typical atrial flutter in association with symptomatic sinus bradycardia at 24 years of age, 7 years following her initial presentation for BBRVT. She was successfully treated with cavotricuspid isthmus ablation and was also noted to have sinus node dysfunction (corrected sinus node recovery time: 2070 ms) at the time of EPS, leading to permanent pacemaker insertion. Fifteen years following her initial presentation, she has had no subsequent arrhythmic events. Case 3 (*LMNA* Leu327Val) developed a dilated cardiomyopathy approximately 6 years following her initial presentation in association with proximal muscle weakness. Despite aggressive intervention including a left ventricular assist device, she died from heart failure while awaiting heart transplantation. Cases 4 and 5, both of whom presented with third degree atrioventricular block, had recovery of atrioventricular conduction during follow-up with <1% ventricular pacing observed on repeated annual pacemaker interrogations. Cases 2 and 6 have had no subsequent arrhythmic episodes during the follow-up period (**Table 1**).

### Genetic Analysis

#### *Case 1*

Next-generation sequencing of the 12 pre-specified genes identified a novel *SCN5A* Ala1905Gly missense mutation (**Table 1**) located on the C-terminus of the ion channel (**Figure**

5). The amino acid was highly conserved among mammalian species (**Supplemental Figure 2a**) and the mutation was predicted to be pathogenic on *in silico* analysis (**Table 1**). Cascade screening of first-degree family members has been offered, but to date has been declined.

#### Case 2

Genetic testing was performed using a commercially available arrhythmia panel (Ambry Genetics, CA, USA) comprised of 29 different genes (**Online Supplement**). The patient was found to carry an *SCN5A* c.4719C>T mutation (**Table 1**) located in exon 27 predicted by two *in silico* splicing tools (Splice Site Prediction by Neural Network, Human Splicing Finder) to generate a cryptic donor splice site located within exon 27 that does not involving the canonical 5' dinucleotide GT donor site. The splice site mutation is predicted to lead to deletion of 32 amino acids from Domain IV of the ion channel (**Figure 5**). *In silico* analysis with Mutation Taster predicted the variant to be “disease causing”. The nucleotide position is highly conserved in mammalian species (**Supplemental Figure 2b**), has previously been reported as the genetic culprit in three separate cases of Brugada syndrome (BrS) (12, 13), and is absent from the Exome Aggregation Consortium database. Another splice site mutation that disrupts the canonical 5' donor splice site of exon 27 resulting in activation of the cryptic splice site at c.4917C has previously been identified in a case of BrS and presence of the aberrant transcript containing the identical 96 base pair deletion predicted to occur secondary to our splice site mutation was demonstrated (14). Electrophysiological studies with patch clamping on the corresponding protein product containing an in-frame 32 amino acid deletion (the identical protein product predicted in our case) revealed a complete loss-of-function (14).

Following identification of the *SCN5A* mutation, modified ECG with precordial leads moved up two intercostal spaces revealed no evidence of a Brugada pattern. Procainamide

challenge was not pursued due to the presence of right bundle branch block following ablation. First-degree relatives have declined subsequent attempts at clinical and genetic cascade screening.

### Case 3

Genetic screening identified a novel *LMNA* Leu327Val mutation (**Table 1 and Supplemental Figure 3**). The amino acid was highly conserved among mammalian species (**Supplemental Figure 2c**) and *in silico* analysis suggested that the mutation was possibly pathogenic (**Table 1**). Family history revealed that the brother of the proband had a pacemaker inserted at 52 years of age for sick sinus syndrome and had mild PR-interval prolongation (210 ms) on surface ECG. To date, genetic and cascade screening of family members has been declined.

### Cases 4, 5, and 6

Next-generation sequencing of the 12 pre-specified genes revealed no rare variants in the remaining cases.

### Electrophysiological Analysis of *SCN5A* Ala1905Gly

The peak current densities of homozygous and heterozygous Ala1905Gly  $\text{Na}_v1.5$  channels in mammalian tsA201 cells were significantly reduced relative to WT ( $p = 0.018$  and  $p = 0.044$ , respectively) (**Table 2 and Figures 6a, 6b, and 6c**). Analysis of gating properties over a wide range of membrane voltages revealed that steady state activation of the homozygous and heterozygous Ala1905Gly  $\text{Na}_v1.5$  currents was shifted significantly to more depolarized membrane potentials relative to WT (**Table 2 and Figure 6d**). Half-maximal activation voltages ( $V_{1/2}$ ) for homozygous and heterozygous Ala1905Gly mutant  $\text{Na}_v1.5$  channels exhibited

statistically significant positive shifts relative to WT ( $p = 0.042$  and  $p = 0.020$ , respectively) (**Table 2**). Evaluation of the inactivation kinetics of the  $\text{Na}_v1.5$  currents revealed that the half-maximal inactivation voltage of the heterozygous and homozygous Ala1905Gly  $\text{Na}_v1.5$  channels differed significantly relative to WT ( $p = 0.002$  and  $p = 0.024$ , respectively) (**Figure 6d** and **Table 2**). The activation slope factor ( $k$ ) was significantly increased in heterozygous Ala1905Gly  $\text{Na}_v1.5$  channels relative to WT ( $p < 0.01$ ), while no differences were observed in inactivation slope factors between mutant and wild-type  $\text{Na}_v1.5$  currents (**Table 2**).

The shifts in steady-state activation and inactivation between mutant and WT  $\text{Na}_v1.5$  channels resulted in a reduced overlap of the activation and inactivation curves resulting in a reduced “window current”. In addition to the fast-recovered inactivation component of steady state inactivation, the slow recovered inactivation component, also referred to as the intermediate inactivation, was also investigated in WT and homozygous Ala1905Gly  $\text{Na}_v1.5$  channels using a two-pulse voltage protocol. The first voltage pulse length was varied from 3 to 3000 ms and was separated from the second voltage pulse by 20 ms of hyperpolarization to -100 mV to permit recovery of the fast inactivation component. The intermediate inactivation of homozygous Ala1905Gly  $\text{Na}_v1.5$  channels ( $0.43 \pm 0.03$ ) was increased compared with the WT  $\text{Na}_v1.5$  channels ( $0.34 \pm 0.03$ ;  $p = 0.035$ ) (**Table 2** and **Supplemental Figure 4**). Inactivation recovery and the late, persistent inward sodium current did not differ significantly in WT and homozygous Ala1905Gly  $\text{Na}_v1.5$  channels (**Table 2** and **Supplemental Figure 5**).

## Discussion

Our investigation into cases of apparent idiopathic BBRVT has identified the first genetic culprits in this life-threatening condition. Pathogenic mutations in 2 separate genes were identified in 3 of 6 individuals, providing evidence to support the use of clinical genetic testing

in cases of idiopathic BBRVT. In addition to establishing idiopathic BBRVT as a genetic condition, our study sheds additional insight into its underlying pathogenesis and emphasizes that conduction system disease in isolation provides a sufficient substrate for arrhythmia development. Our findings also highlight BBRVT as a novel genetic etiology of unexplained sudden cardiac death among individuals with structurally normal hearts. The latter further emphasizes the important role for EPS in the evaluation and management of cases of aborted cardiac arrest, a particularly important concept given that BBRVT can be cured with catheter ablation.

The findings from our study implicate both *SCN5A* and *LMNA* as genetic culprits of BBRVT. Case 1 possessed a novel *SCN5A* mutation in a highly conserved residue (Ala1905Gly) located on the C-terminus of the ion channel (**Figure 5**). Findings from *in vitro* electrophysiological analyses revealed that, relative to wild-type  $\text{Na}_v1.5$  current, homozygous and heterozygous Ala1905Gly mutants had reduced peak current densities and steady state activation and half-maximal activation voltages that were significantly shifted to more depolarized membrane potential. Collectively, these findings were consistent with the *SCN5A* Ala1905Gly missense variant being a pathogenic loss-of-function mutation that was causative for the constellation of clinical arrhythmias in Case 1, including BBRVT, cardiac conduction system disease, atrial flutter, and sinus node dysfunction.

Case 2 possessed an *SCN5A* c.4719C>T mutation located in exon 27 predicted to result in activation of a cryptic 5' donor splice site leading to loss of 96 nucleotides from the mRNA product. This nucleotide is highly conserved among mammalian species (**Supplemental Figure 1b**) and has been reported as the genetic culprit in 3 cases of BrS (12, 13). The impact of the aberrant splicing is a 32 amino acid in-frame deletion involving the S2/S3 segments and

intervening cytoplasmic loop of Domain IV (**Figure 5**). Previous functional work on another splice-site mutation disrupting the 5' donor site at the distal end of exon 27 and resulting in the identical 32 amino acid in-frame deletion revealed a complete loss-of-function, consistent with it being pathogenic (14).

Notably, case 2 did not have ECG findings of BrS with surface leads in the standard and modified high positions, while a procainamide challenge was not performed due to the presence of right bundle branch block following ablation (15). Identification of an identical mutation causing two different phenotypes, termed genetic pleiotropy, is a common finding with *SCN5A* (16, 17). In reference to BrS, it should also be noted that affected patients often have conduction system disease, as evidenced by prolonged HV-intervals at the time of EPS (18). Although ventricular arrhythmias in BrS are almost exclusively polymorphic, in rare instances when monomorphic VT is observed, consideration should be given to BBRVT as a potential underlying etiology, as highlighted by a recent study (19, 20).

The *LMNA* gene encodes both the lamin A and C proteins, generated through alternative splicing, that are constituents of nuclear lamina that reside immediately inside the inner nuclear membrane (**Supplemental Figure 3**) (21). In the context of cardiac disease, *LMNA* mutations most often cause an autosomal dominant form of dilated cardiomyopathy associated with conduction system disease (22). A select group of other genetic dilated cardiomyopathies are also linked to conduction system disease, including those associated with the *PRKAG2*, *TBX5*, and *NKX2-5* genes, and both phenotypic features most often develop concomitantly (23–25). Our patient presented with underlying conduction system disease and BBRVT prior to subsequently developing dilated cardiomyopathy. The *LMNA* Leu327Val mutation is novel and the phenotype of the proband, which included conduction system disease, atrial fibrillation,

subsequent development of cardiomyopathy (following onset of BBRVT), and proximal muscle weakness, is classic for a laminopathy, lending support for the identified mutation being the genetic culprit.

The dramatic presentations of our cases, including syncope and cardiac arrests requiring resuscitation secondary to heart rates frequently exceeding 200bpm, also emphasize the malignant potential of BBRVT. Our findings highlight that BBRVT should be considered as a potential culprit in cases of unexplained sudden cardiac death, a concept that is generally not incorporated in diagnostic algorithms for this patient population (26–28). The need to screen for BBRVT highlights the critical importance of invasive EPS, particularly when there is evidence of underlying conduction system disease on surface ECG. Owing to the dependence of BBRVT on the specialized conduction system, these induction protocols should always include long-short extra-stimuli. In addition to facilitating accurate diagnosis, catheter ablation can also serve as a curative therapy for this life-threatening arrhythmia, particularly notable given that none of the other causes of unexplained aborted cardiac arrest in this patient population can be cured. That being said, implantation of an ICD is still likely reasonable given that the genetic mutation may potentially lead to additional cardiac abnormalities that continue to place patients at risk of sudden cardiac death. Both patients in this study that suffered aborted cardiac arrests were offered ICDs, though Case 2 declined.

Among the remaining cases of BBRVT in our cohort, the inability to identify an underlying genetic etiology may be secondary to the presence of undiscovered genetic culprits or a non-genetic mechanism for their underlying conduction system disease. Although we excluded cases of known myocarditis, it is notable that Cases 4 & 5 appeared to recover atrioventricular conduction during follow-up, as evidenced by their requiring less than 1% ventricular pacing



after 1 year of follow-up. It is conceivable that their conduction system disease may have been secondary to a focal myocarditis that subsequently resolved. The third degree atrioventricular block and distal conduction system disease observed in Cases 4 and 5 could also have been secondary to Lev's disease that may have developed in association with their bicuspid aortic valves, particularly for Case 5, whose aortic valve was heavily calcified (29). Although conceivable, Lev's disease is generally progressive, while the atrioventricular block in both of these patients resolved during follow-up. Analogous to heart block among young individuals (30), it is probable that BBRVT in the setting of structurally normal hearts may have multiple etiologies.

### Limitations

Although our study examining BBRVT in the absence of structural heart disease involves the largest case series to date, being drawn from 6 North American centers, our study size of 6 patients is modest. The primary goal of this investigation was to identify novel genetic culprits and, as highlighted by our novel findings, the cohort was sufficient to accomplish this goal. A larger sample size will be necessary to more definitively establish the prevalence of genetic mutations in this patient population. The families of each proband found to carry a presumed pathogenic mutation have declined cascade screening, which has precluded evaluation for genotype-phenotype segregation. Although this may be viewed as a limitation for definitively concluding that the identified mutations were the genetic culprits for the BBRVT phenotype, for both *SCN5A* mutations, we provided multiple lines of *in silico* and *in vitro* evidence consistent with their being pathogenic. Support for the novel *LMNA* mutation being pathogenic was provided by the clinical phenotype being classic for a laminopathy.

### Conclusions

Our investigation into BBRVT in the setting of normal biventricular size and systolic function has identified the first genetic culprits for this life-threatening ventricular arrhythmia. Identification of culprit mutations within *SCN5A* and *LMNA* provides further insight into the pathophysiology underlying the condition and emphasizing a potential role for routine clinical genetic testing for idiopathic BBRVT. Our findings also highlight BBRVT as a novel genetic etiology of unexplained sudden cardiac death that can be cured with catheter ablation. Clinical Perspectives

**Competency in Medical Knowledge:** Bundle branch reentrant ventricular tachycardia may have an underlying genetic origin and is a novel genetic etiology of unexplained sudden cardiac death. Genetic testing of the *SCN5A* and *LMNA* genes should be considered among patients with bundle branch reentrant ventricular tachycardia in the setting of a structurally normal heart. Survivors of unexplained sudden cardiac death should be considered for an invasive electrophysiology study that includes long-short extra-stimuli during the induction protocol to screen for bundle branch reentrant ventricular tachycardia.

**Translational Outlook:** The role of genetics in bundle branch reentrant ventricular tachycardia associated with structural heart disease is unknown and should be investigated in future studies. The prevalence of bundle branch reentrant ventricular tachycardia among survivors of unexplained sudden cardiac death should be evaluated to further clarify the role of invasive electrophysiology study among this patient population.

## References

1. Blanck Z, Dhala A, Deshpande S, Sra J, Jazayeri M, Akhtar M. Bundle branch reentrant ventricular tachycardia: cumulative experience in 48 patients. *J. Cardiovasc. Electrophysiol.* 1993;4:253–262.
2. Akhtar M, Gilbert C, Wolf FG, Schmidt DH. Reentry within the His-Purkinje system. Elucidation of reentrant circuit using right bundle branch and His bundle recordings. *Circulation* 1978;58:295–304.
3. Caceres J, Jazayeri M, McKinnie J, et al. Sustained bundle branch reentry as a mechanism of clinical tachycardia. *Circulation* 1989;79:256–270.
4. Blanck Z, Jazayeri M, Dhala A, Deshpande S, Sra J, Akhtar M. Bundle branch reentry: a mechanism of ventricular tachycardia in the absence of myocardial or valvular dysfunction. *J. Am. Coll. Cardiol.* 1993;22:1718–1722.
5. Simons GR, Sorrentino RA, Zimmerman LI, Wharton JM, Natale A. Bundle branch reentry tachycardia and possible sustained interfascicular reentry tachycardia with a shared unusual induction pattern. *J. Cardiovasc. Electrophysiol.* 1996;7:44–50.
6. Baruteau A-E, Behaghel A, Fouchard S, et al. Parental electrocardiographic screening identifies a high degree of inheritance for congenital and childhood nonimmune isolated atrioventricular block. *Circulation* 2012;126:1469–1477.
7. Wolf CM, Berul CI. Inherited conduction system abnormalities--one group of diseases, many genes. *J. Cardiovasc. Electrophysiol.* 2006;17:446–455.

8. Baruteau A-E, Probst V, Abriel H. Inherited progressive cardiac conduction disorders. *Curr. Opin. Cardiol.* 2015;30:33–39.
9. Hoffmayer KS, Yang Y, Joseph S, et al. Predictors of unusual ECG characteristics in cavotricuspid isthmus-dependent atrial flutter ablation. *Pacing Clin. Electrophysiol.* 2011;34:1251–1257.
10. Sung RK, Kim AM, Tseng ZH, et al. Diagnosis and ablation of multiform fascicular tachycardia. *J. Cardiovasc. Electrophysiol.* 2013;24:297–304.
11. Guerrero MA, Zhu DW, Zakharova MY, Nelson WB. Bundle Branch Re-entry Ventricular Tachycardia Storm During the Recovery Phase of Transient Complete Heart Block. *Journal of Innovations in Cardiac Rhythm Management.* 2013;4:1461-69.
12. Amin AS, de Groot EAA, Ruijter JM, Wilde AAM, Tan HL. Exercise-induced ECG changes in Brugada syndrome. *Circ. Arrhythm. Electrophysiol.* 2009;2:531–539.
13. Amin AS, Boink GJJ, Atrafi F, et al. Facilitatory and inhibitory effects of SCN5A mutations on atrial fibrillation in Brugada syndrome. *Europace.* 2011;13:968–975.
14. Hong K, Guerchicoff A, Pollevick GD, et al. Cryptic 5' splice site activation in SCN5A associated with Brugada syndrome. *J. Mol. Cell. Cardiol.* 2005;38:555–560.
15. Aizawa Y, Takatsuki S, Sano M, et al. Brugada syndrome behind complete right bundle-branch block. *Circulation* 2013;128:1048–1054.
16. Remme CA, Wilde AAM, Bezzina CR. Cardiac sodium channel overlap syndromes: different faces of SCN5A mutations. *Trends Cardiovasc. Med.* 2008;18:78–87.

17. Kyndt F, Probst V, Potet F, et al. Novel SCN5A mutation leading either to isolated cardiac conduction defect or Brugada syndrome in a large French family. *Circulation* 2001;104:3081–3086.
18. Alings M, Wilde A. “Brugada” Syndrome Clinical Data and Suggested Pathophysiological Mechanism. *Circulation* 1999;99:666–673.
19. Mazur A, Iakobishvili Z, Kusniec J, Strasberg B. Bundle branch reentrant ventricular tachycardia in a patient with the Brugada electrocardiographic pattern. *Ann. Noninvasive Electrocardiol.* 2003;8:352–355.
20. Rodríguez-Mañero M, Sacher F, de Asmundis C, et al. Monomorphic ventricular tachycardia in patients with Brugada syndrome: A multicenter retrospective study. *Heart Rhythm.* 2016;13:669–682.
21. Worman HJ, Fong LG, Muchir A, Young SG. Laminopathies and the long strange trip from basic cell biology to therapy. *J. Clin. Invest.* 2009;119:1825–1836.
22. Fatkin D, MacRae C, Sasaki T, et al. Missense mutations in the rod domain of the lamin A/C gene as causes of dilated cardiomyopathy and conduction-system disease. *N. Engl. J. Med.* 1999;341:1715–1724.
23. Gollob MH, Green MS, Tang AS, et al. Identification of a gene responsible for familial Wolff-Parkinson-White syndrome. *N. Engl. J. Med.* 2001;344:1823–1831.
24. Basson CT, Bachinsky DR, Lin RC, et al. Mutations in human TBX5 [corrected] cause limb and cardiac malformation in Holt-Oram syndrome. *Nat. Genet.* 1997;15:30–35.

25. Schott JJ, Benson DW, Basson CT, et al. Congenital heart disease caused by mutations in the transcription factor NKX2-5. *Science* 1998;281:108–111.
26. Krahn AD, Healey JS, Chauhan V, et al. Systematic assessment of patients with unexplained cardiac arrest: Cardiac Arrest Survivors With Preserved Ejection Fraction Registry (CASPER). *Circulation* 2009;120:278–285.
27. Behr ER, Dalageorgou C, Christiansen M, et al. Sudden arrhythmic death syndrome: familial evaluation identifies inheritable heart disease in the majority of families. *Eur. Heart J.* 2008;29:1670–1680.
28. Tan HL, Hofman N, van Langen IM, van der Wal AC, Wilde AAM. Sudden unexplained death: heritability and diagnostic yield of cardiological and genetic examination in surviving relatives. *Circulation* 2005;112:207–213.
29. Lev M. Anatomic Basis For Atrioventricular Block. *Am. J. Med.* 1964;37:742–748.
30. Kandolin R, Lehtonen J, Kupari M. Cardiac Sarcoidosis and Giant Cell Myocarditis as Causes of Atrioventricular Block in Young and Middle-Aged Adults. *Circ. Arrhythm. Electrophysiol.* 2011;4:303–309.

## **Figure Legends**

**Figure 1:** Bundle Branch Re-entrant Ventricular Tachycardia (BBRVT) Circuit with Surface ECG and Intra-cardiac Findings. (A) Illustrates a BBRVT circuit with antegrade conduction down the right bundle and retrograde conduction along the left bundle resulting in a surface ECG with a left bundle branch block morphology. (B) Illustrates a BBRVT circuit with antegrade conduction down the left bundle and retrograde conduction along the right bundle resulting in a surface ECG with a right bundle branch block morphology. (C) Intra-cardiac tracing of BBRVT revealing the His-His interval preceding and predicting the subsequent Ventricular-Ventricular interval.

H = His, V = Ventricular

**Figure 2:** QRS complex on surface ECGs in the absence of BBRVT in Cases 1, 2, 3, and 6.

**Figure 3:** Atrioventricular block associated with an infra-nodal escape observed on presentation in Cases 4 (top) and 5 (bottom).

**Figure 4:** Intracardiac electrograms demonstrating (A) a long-short initiation of BBRVT via pacing from the right ventricle, (B) variations in right bundle (RB) to RB potential intervals preceding and predicting variations in ventricular to ventricular activation intervals.

H = His potential, A = atrial electrogram, V = ventricular.

**Figure 5:** *SCN5A* c.4719 C>T Mutation Results in Aberrant Splicing and a 32 Amino Acid In-Frame Deletion in Domain IV of the Ion Channel. *SCN5A* Ala1905Gly resides within the C-terminus of the ion channel.

**Figure 6:** Biophysical properties of wild-type and mutant Ala1905Gly  $\text{Na}_v1.5$  currents expressed in tsA201 cells. (A) Whole cell currents of wild-type, homozygous, and heterozygous Ala1905Gly  $\text{Na}_v1.5$  channels. (B) Peak currents of mutant  $\text{Na}_v1.5$  channels were significantly

reduced relative to wild-type. (C) Current-voltage relationships revealed significant reductions in current densities of homozygous and heterozygous Ala1905Gly Na<sub>v</sub>1.5 channels relative to wild-type at multiple different membrane voltages. (D) Steady-state voltage-dependent properties of activation and inactivation for wild-type, homozygous, and heterozygous Ala1905Gly Na<sub>v</sub>1.5 channels.

pA = picoamperes, wt = wild-type, pF = picofarad, \* =  $p < 0.05$ , \*\* =  $p < 0.01$ , mV = millivolts



**Table 1:** Clinical, Electrophysiologic, and Genetic Features of Bundle Branch Reentrant Ventricular Tachycardia Study Participants.

F=female, M=male, CCD=cardiac conduction system disease, ACA=aborted cardiac arrest,

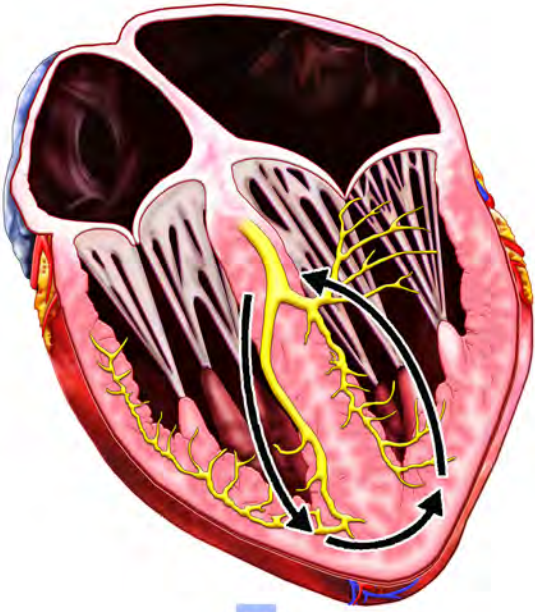
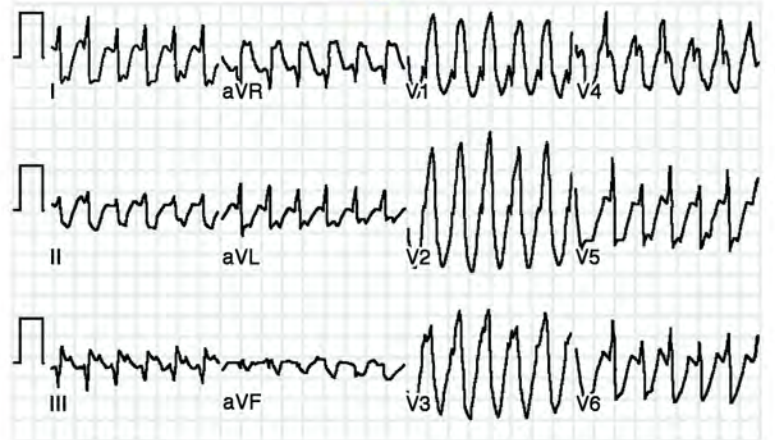
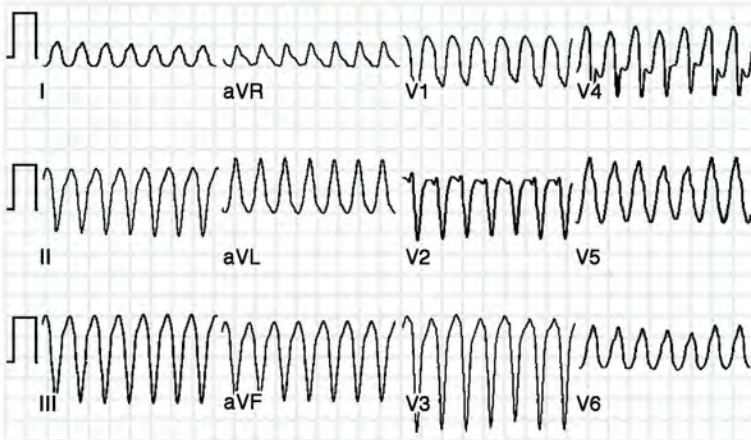
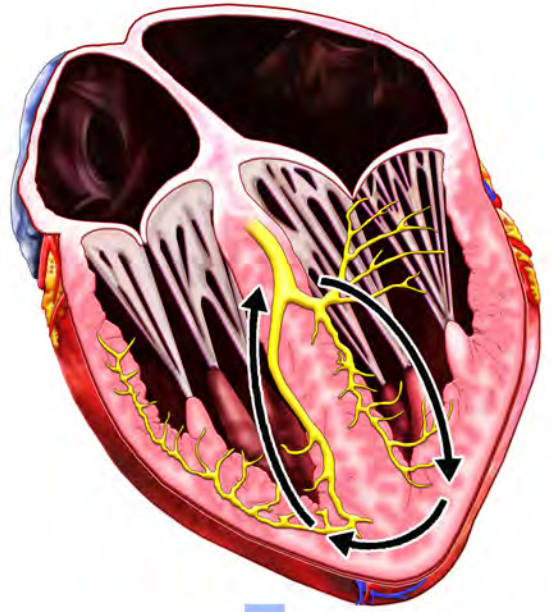
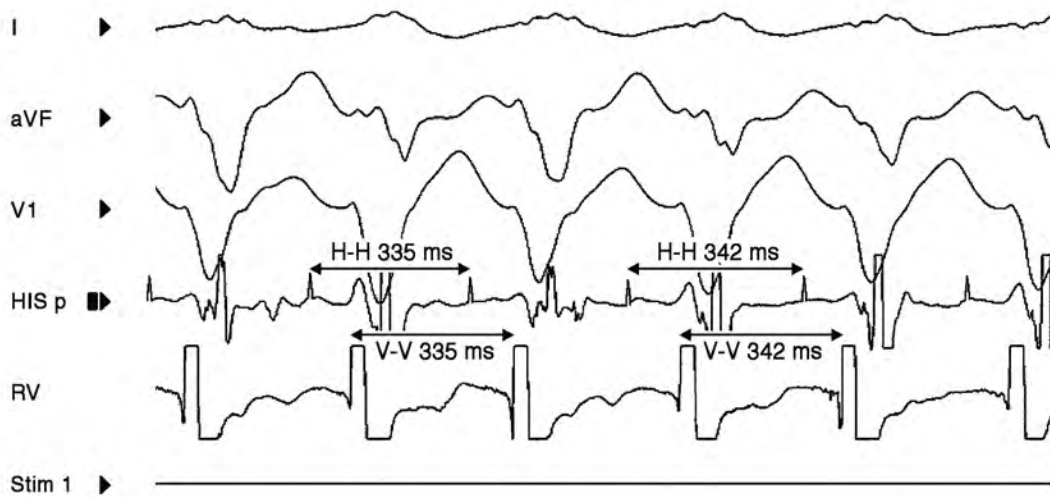
	Cases					
	1	2	3	4	5	6
<b>Clinical Features</b>						
<b>Age at Diagnosis (years)</b>	17	18	38	37	22	29
<b>Gender</b>	F	M	F	M	M	M
<b>Family History</b>	Nil	Nil	CCD	Nil	Nil	Nil
<b>Presentation</b>	ACA	Syncope	ACA	Pre-syncope	Syncope	Palpitations
<b>Structural Heart Disease</b>	Nil	Nil	BAE	BAV	BAV	Nil
<b>Arrhythmia Features</b>						
<b>Presenting Rhythm</b>	BBRVT	BBRVT	BBRVT	AVB	AVB	BBRVT
<b>Baseline ECG</b>	QRS 120 ms	Indet axis	AF & LBBB	AVB	AVB	iRBBB
<b>Baseline HV (ms)</b>	61	79	62	60	78	75
<b>BBRVT Morphology</b>	R & LBBB	LBBB	LBBB	LBBB	R & LBBB	LBBB
<b>BBRVT HV (ms)</b>	74	91	75	66	86	115
<b>BBRVT Rate (bpm)</b>	260, 240	170	250	200	270, 230	220
<b>Follow-Up Years</b>	15	3	8	3	4	7
<b>Other Arrhythmias</b>	SND, AF1	Nil	Nil	Nil	Nil	Nil
<b>Clinical Status</b>	Alive	Alive	Deceased	Alive	Alive	Alive
<b>Genetic Mutation</b>						
<b>Gene</b>	SCN5A	SCN5A	LMNA	-	-	-
<b>Nucleotide Change</b>	C > G	C > T	C > G	-	-	-
<b>Mutation Type</b>	Missense	Splice Site	Missense	-	-	-
<b>Amino Acid Change</b>	Ala1905Gly	N/A	Leu327Val	-	-	-
<b>In Silico Analysis</b>						
<b>PolyPhen-2 Score</b>	0.999	N/A	0.566	-	-	-
<b>SIFT Score</b>	0	N/A	0.05	-	-	-
<b>Mutation Taster Score</b>	Disease Causing	Disease Causing	Disease Causing	-	-	-

BAE=biatrial enlargement, BAV=bicuspid aortic valve, BBRVT=bundle branch reentrant ventricular tachycardia, Indet axis = indeterminate axis, AVB= third degree atrioventricular block, NIVCD=non-specific intra-ventricular conduction delay, AF=atrial fibrillation, iRBBB = incomplete right bundle branch block, HV=His-ventricular, ms = milliseconds, LBBB=left bundle branch block, bpm=beats per minute, SND=sinus node dysfunction, AF1=atrial flutter.

**Table 2:** Peak Current and Kinetics of Activation and Inactivation in Wild-Type and Mutant Ala1905Gly Na<sub>v</sub>1.5 Currents

	Na <sub>v</sub> 1.5		
	wt	Ala1905Gly	wt/Ala1905Gly
<b><i>I</i><sub>peak</sub> (pA/pF)</b>	-263.3 ± 40.5	-144.3 ± 21.4*	-164.8 ± 21.4*
<b>Activation Kinetics</b>			
<b><i>V</i><sub>1/2</sub> (mV)</b>	-45.0 ± 1.8	-39.9 ± 1.6*	-39.7 ± 1.2*
<b>Slope Factor (k)</b>	2.3 ± 0.4	3.2 ± 0.4	4.3 ± 0.3**
<b>Inactivation Kinetics</b>			
<b><i>V</i><sub>1/2</sub> (mV)</b>	-72.0 ± 1.1	-76.2 ± 1.3*	-80.0 ± 1.1*
<b>Slope Factor (k)</b>	-8.8 ± 1.8	-6.6 ± 0.5	-5.8 ± 0.9
<b><math>\tau_f</math> (ms)</b>	13.2 ± 1.4	14.2 ± 1.2	-
<b><math>\tau_s</math> (ms)</b>	157.4 ± 38.3	119.4 ± 24.8	-
<b><i>I</i><sub>intermediate inact</sub></b>	0.34 ± 0.03	0.43 ± 0.03*	-
<b><i>I</i><sub>sus</sub></b>	0.12 ± 0.04	0.12 ± 0.06	-

\*p < 0.05 and \*\*p < 0.01 relative to the wild-type, wt = wild-type, *I*<sub>peak</sub> = peak current density, pA/pF = picoamperes per picofarad, *V*<sub>1/2</sub> = half-maximal voltage of activation or inactivation, mV = millivolts,  $\tau_f$  = time constant of fast inactivation recovery,  $\tau_s$  = time constant of slow inactivation recovery, *I*<sub>intermediate inact</sub> = intermediate inactivation, *I*<sub>sus</sub> = sustained current; also referred to as late, persistent inward sodium current.

**A****B****C**

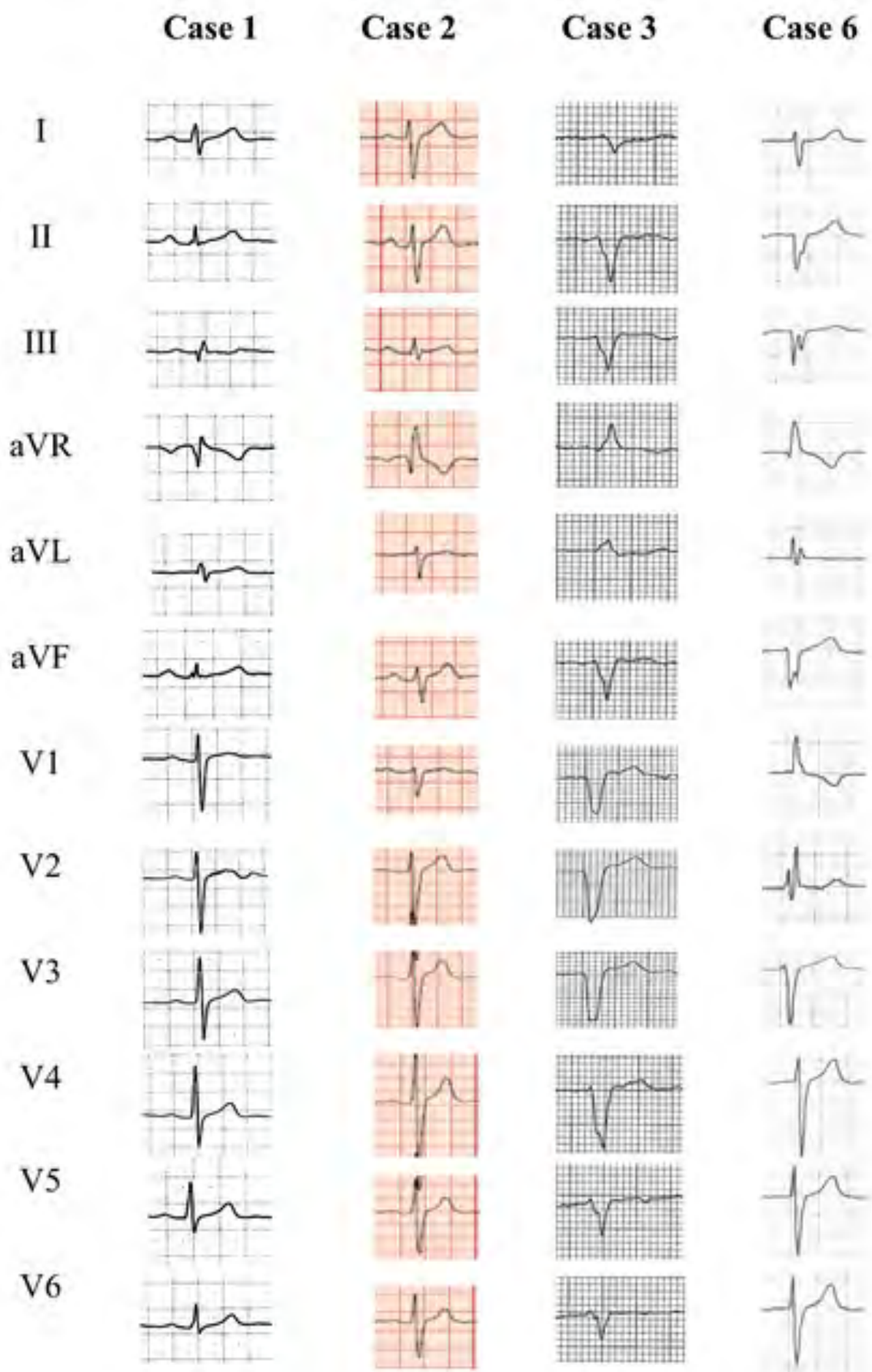


# Figure 3a

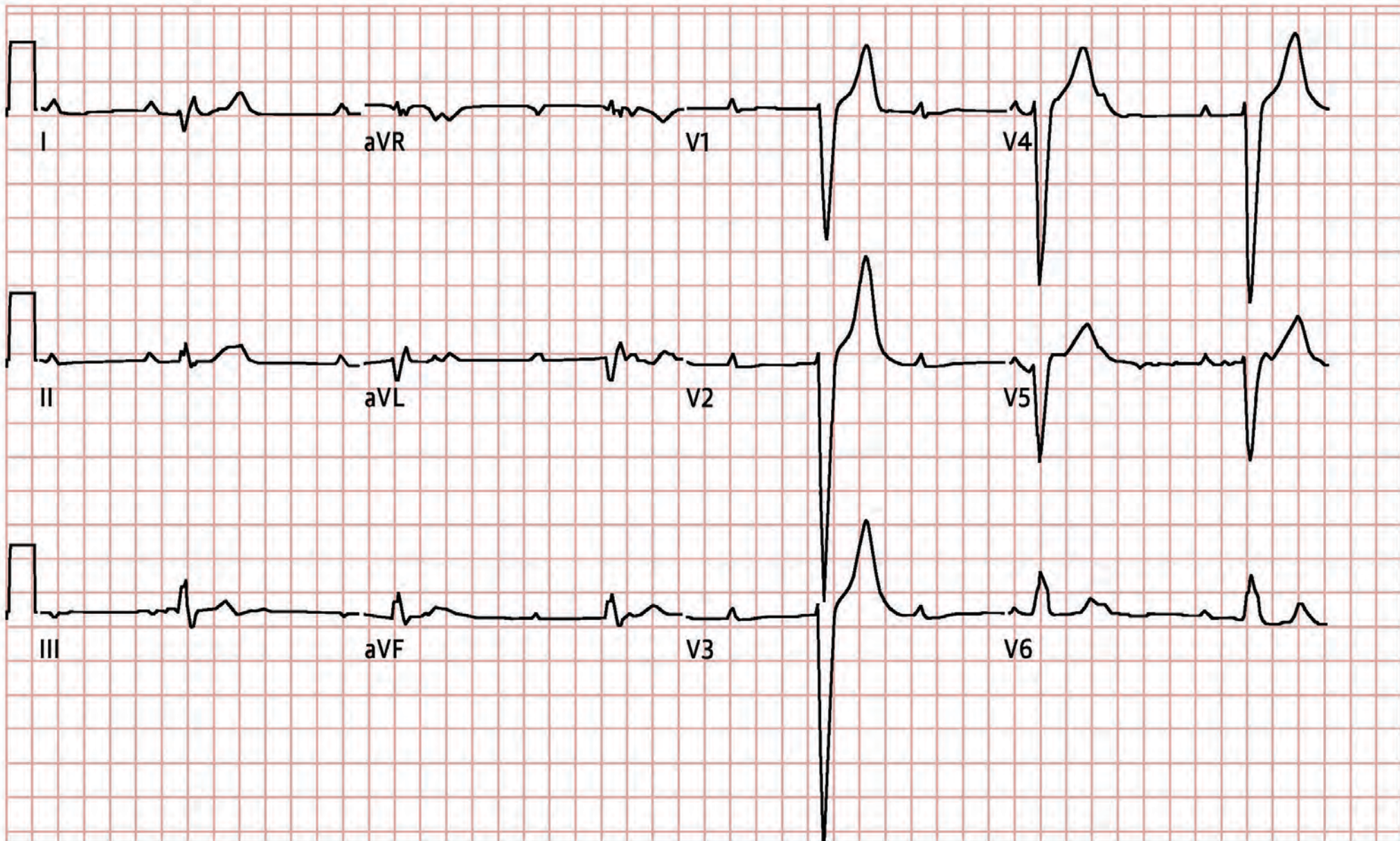


# Figure 3b

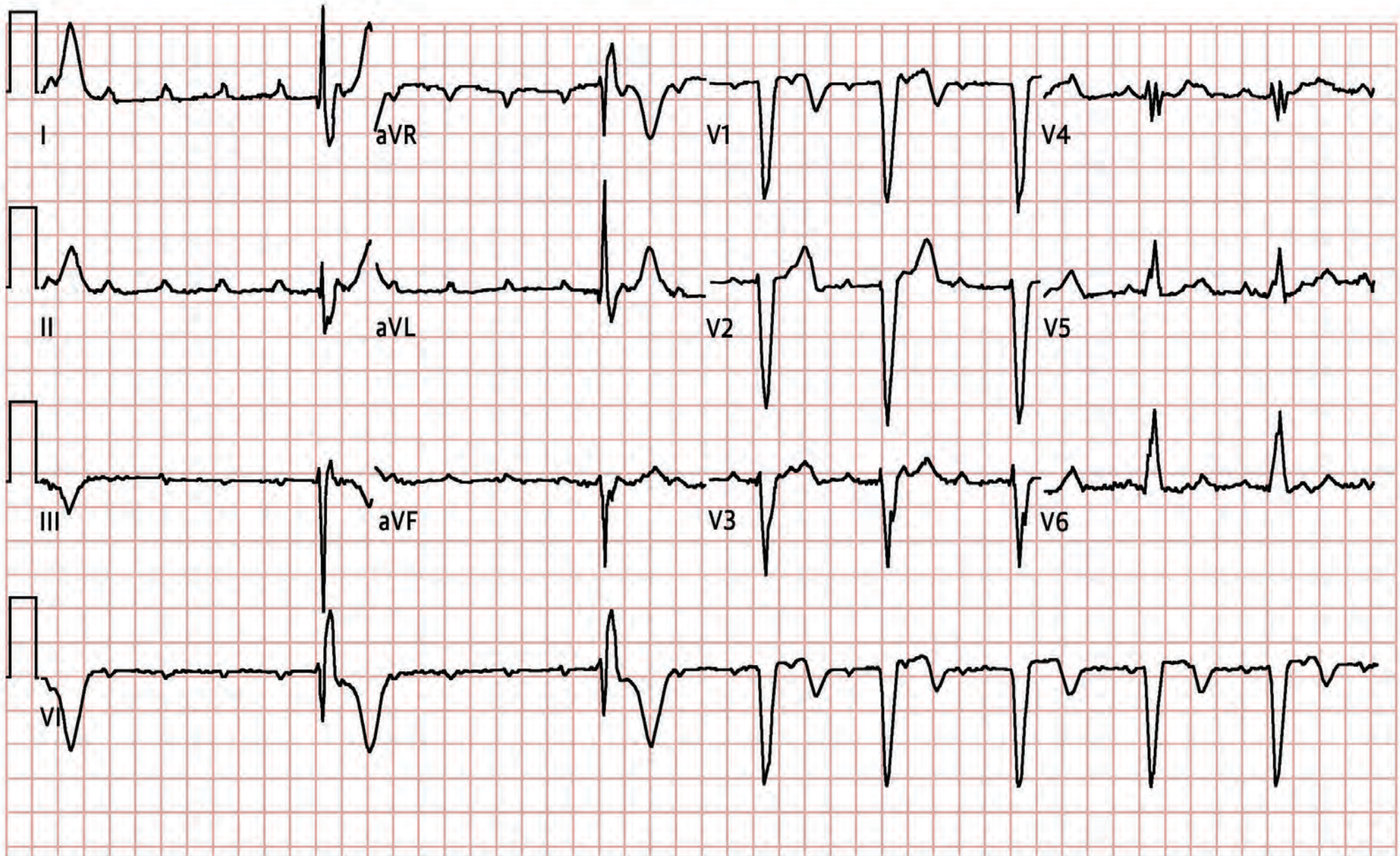


# Figure 4a

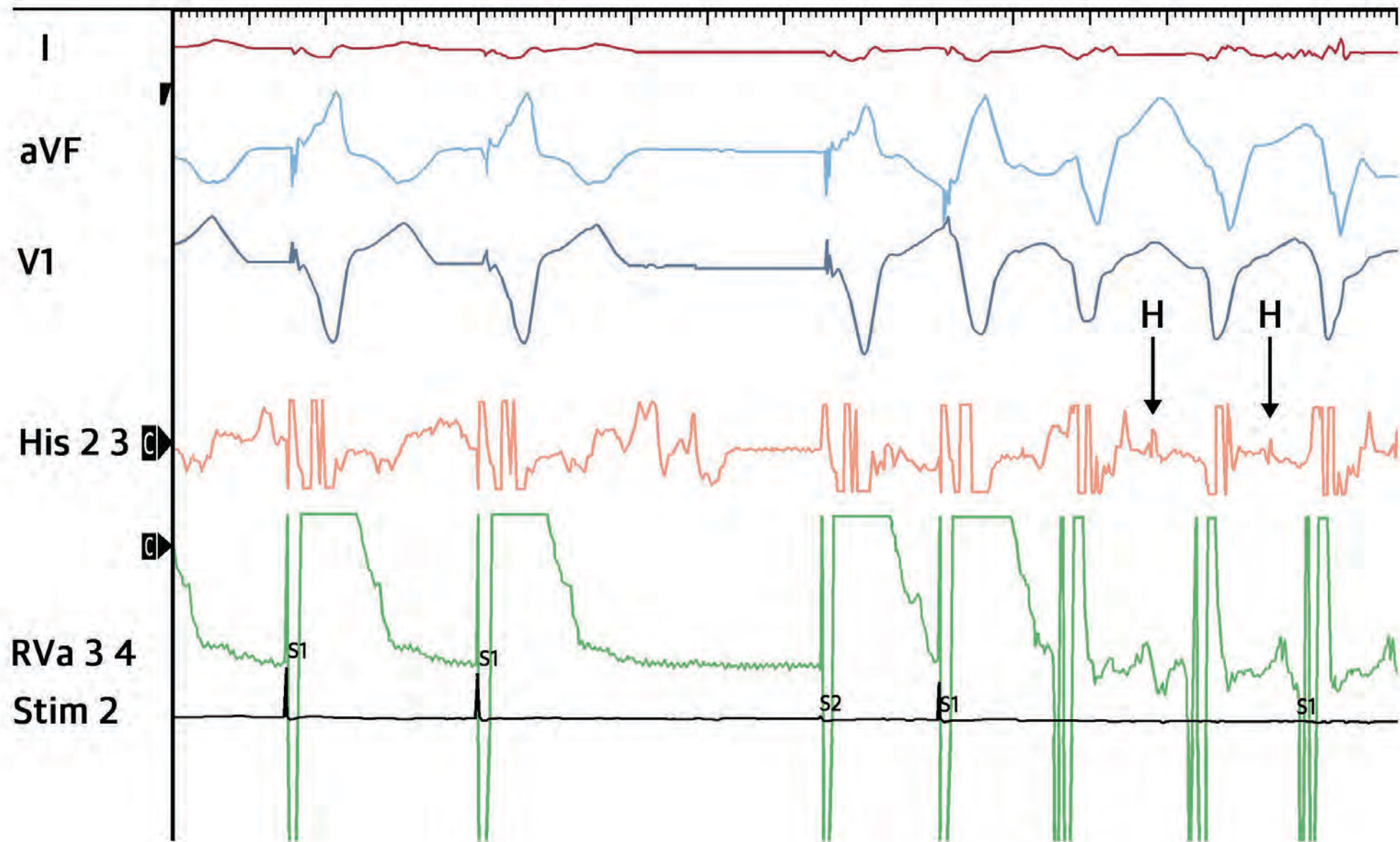
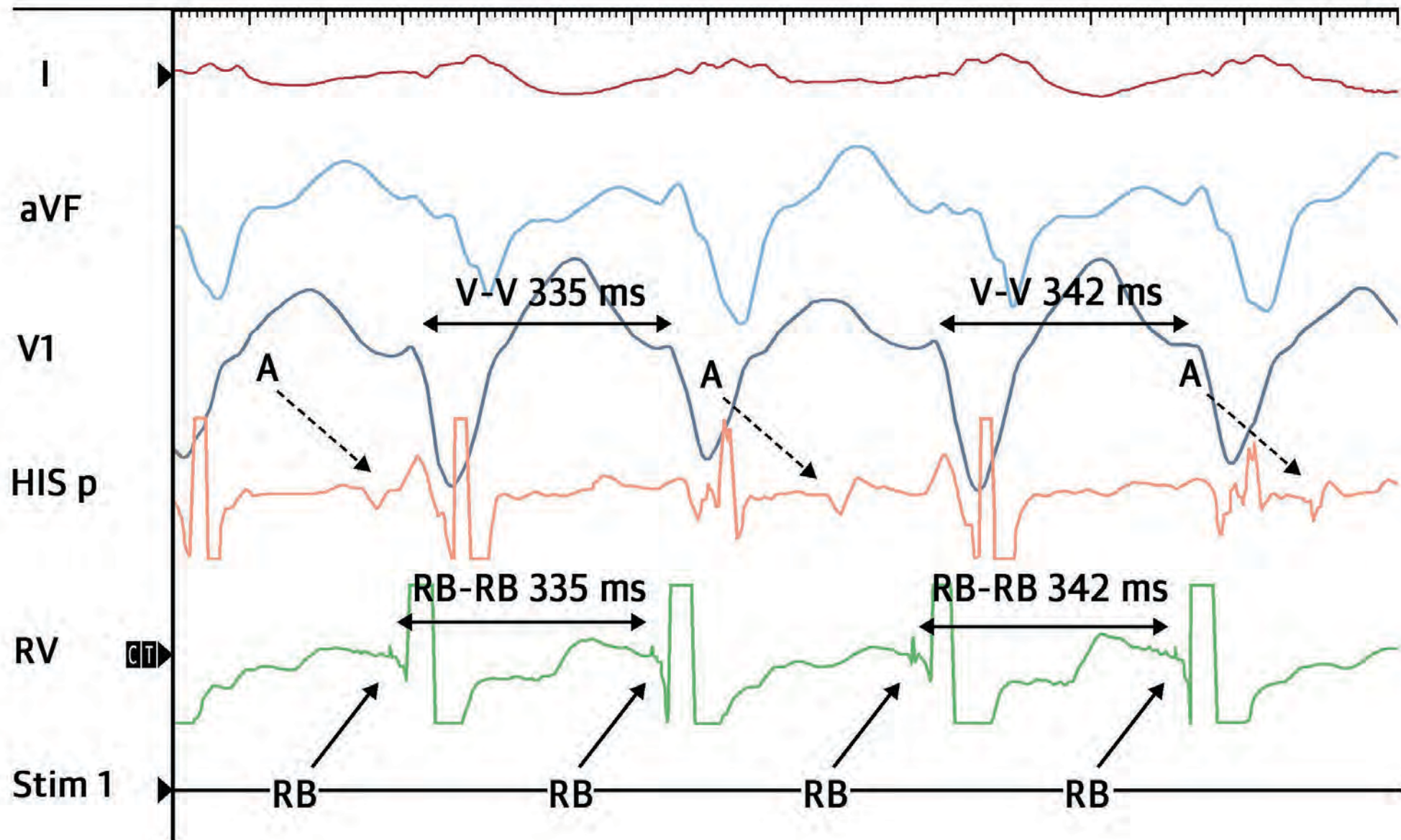


# Figure 4b





# SCN5A Gene Size: 28 Exons

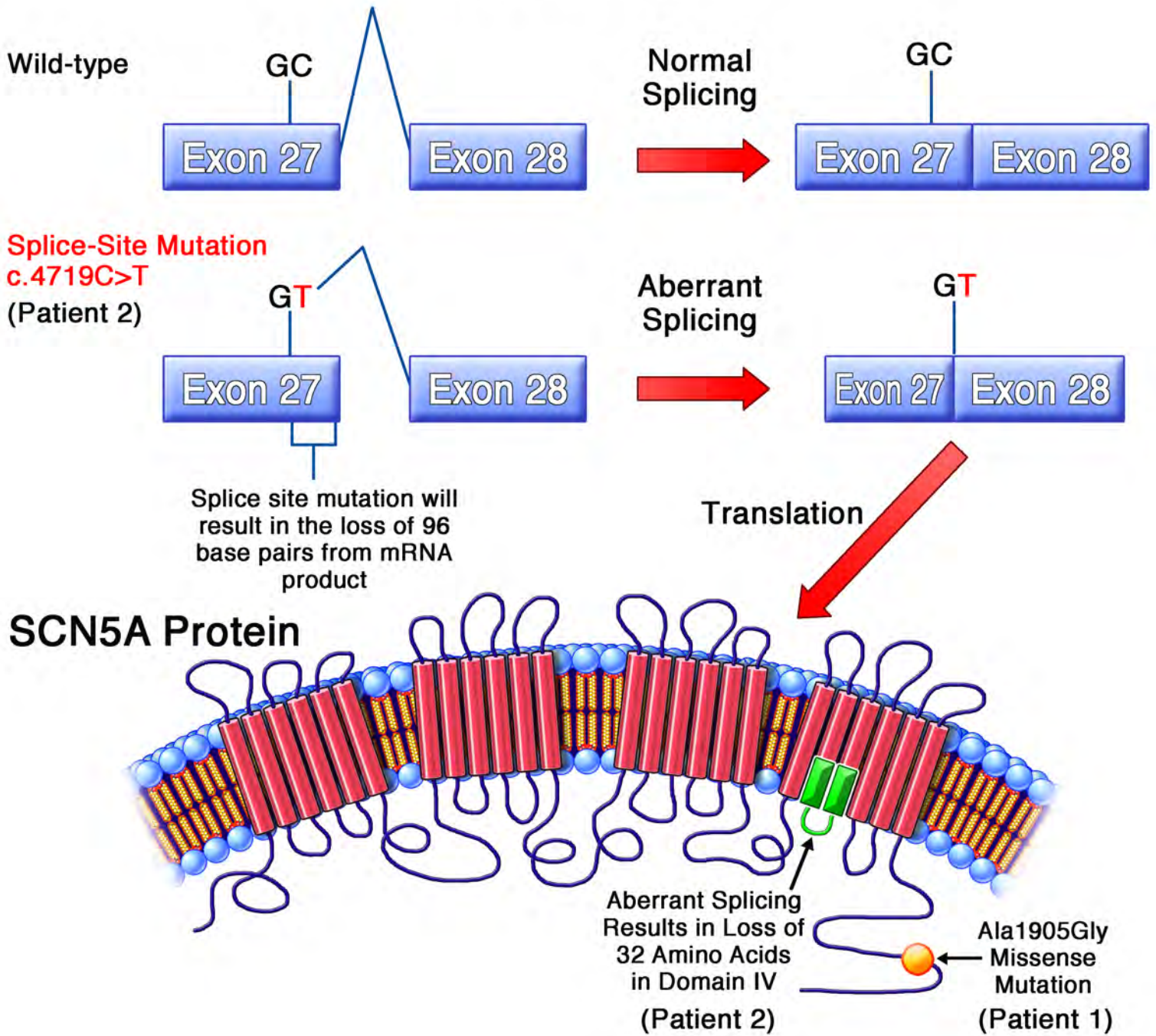
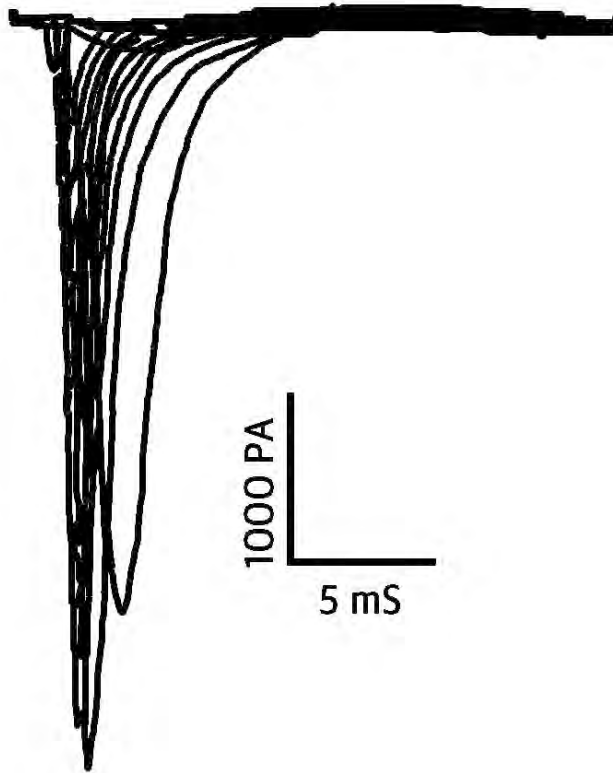
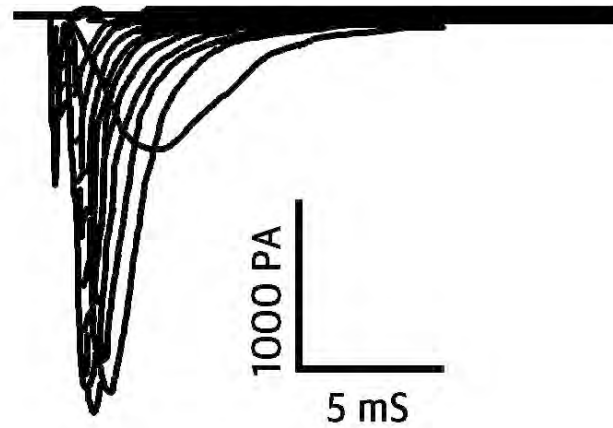


# Figure 6a

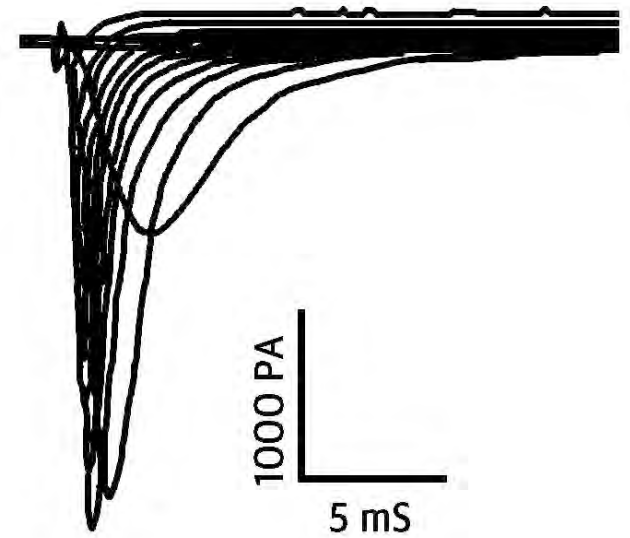
Na<sub>v</sub>1.5 wt



Na<sub>v</sub>1.5 Ala1905Gly



Na<sub>v</sub>1.5 wt + Ala1905Gly



+50 mV

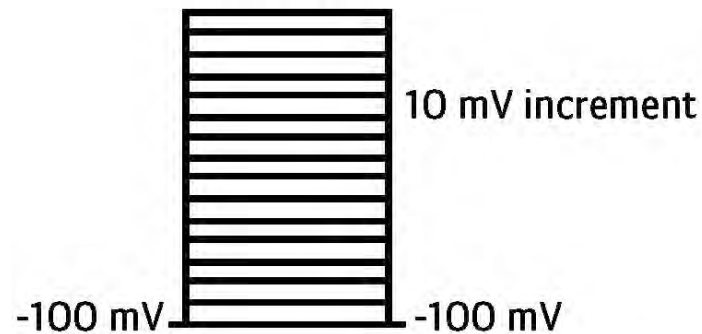


# Figure 6b

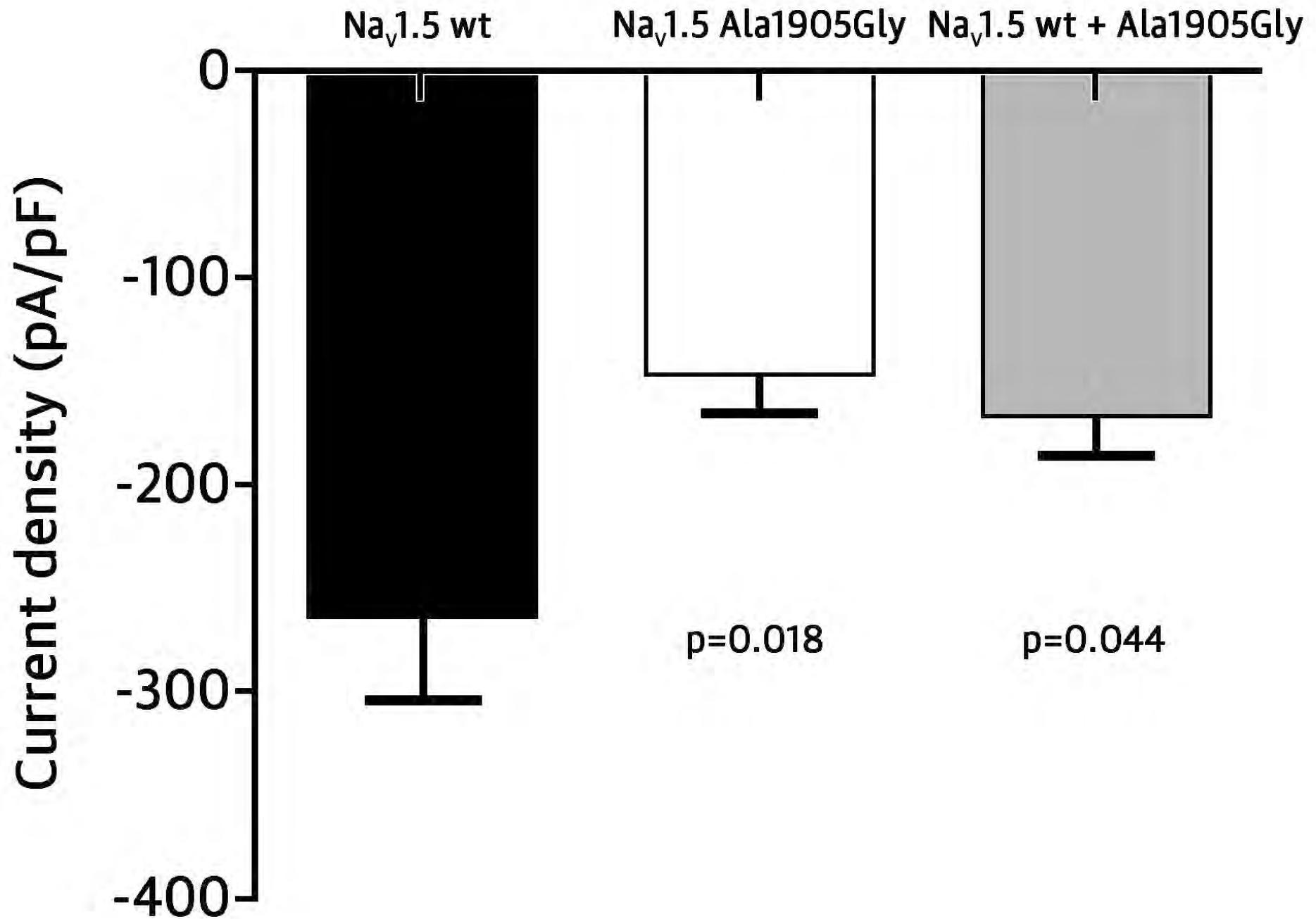


# Figure 6c

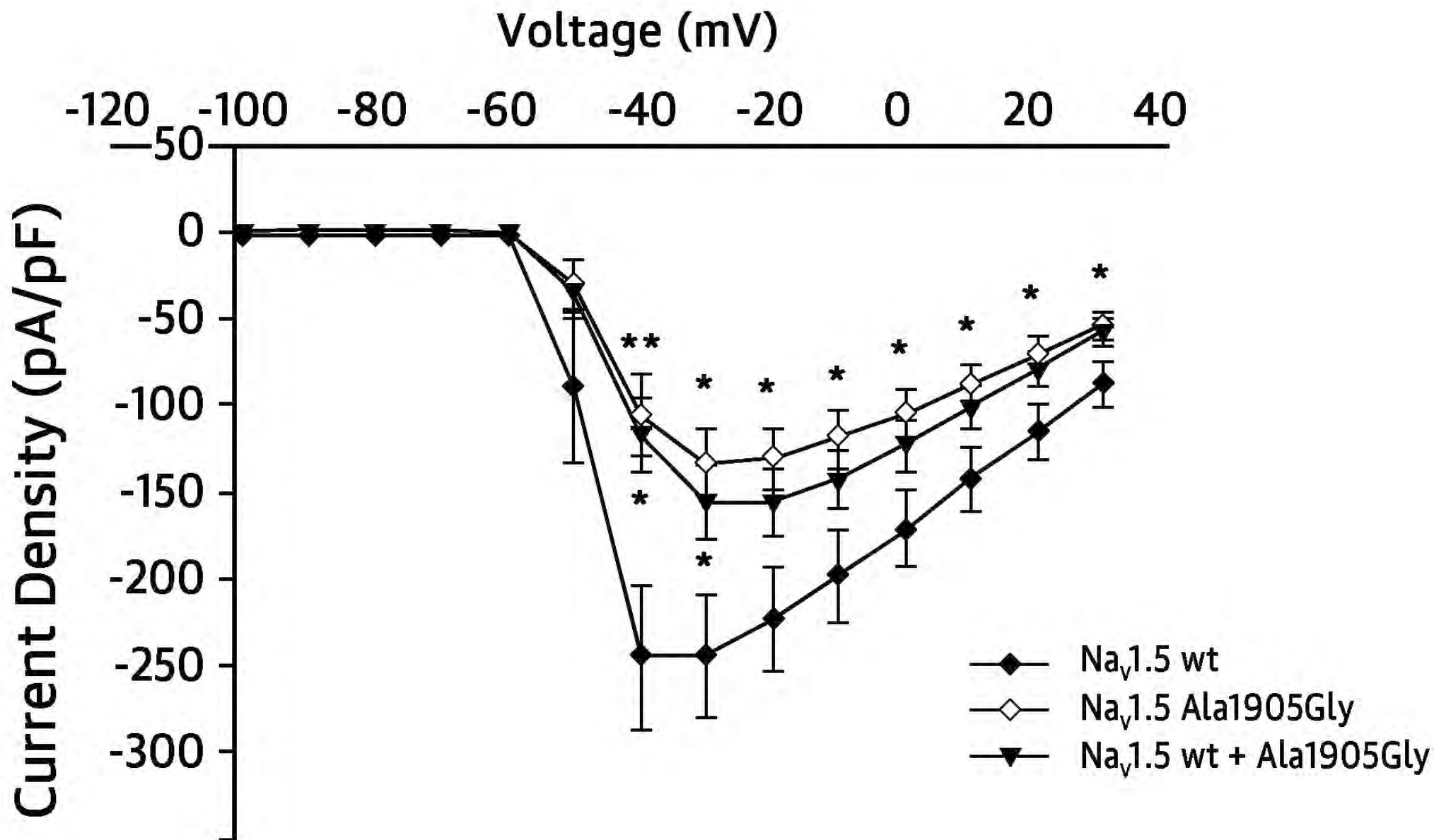


# Figure 6d

